

Supporting Information

Dirhodium complexes: determination of absolute configuration by exciton chirality method using VCD spectroscopy

Gábor Szilvágyi,^a Balázs Brém,^b Gábor Báti,^a László Tölgyesi,^c Miklós Hollósi,^a Elemér Vass^{a*}

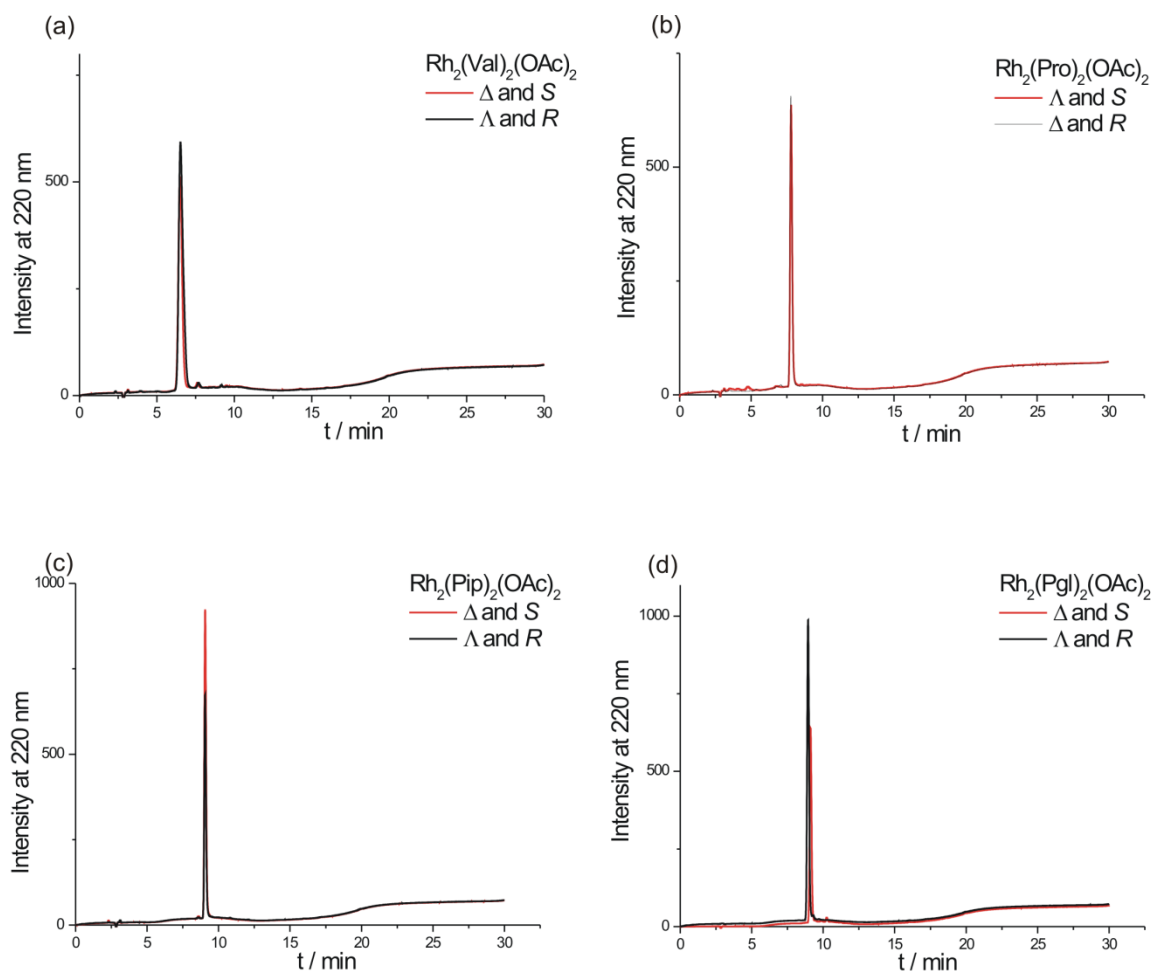


Figure S1. The chromatograms of the purified complexes

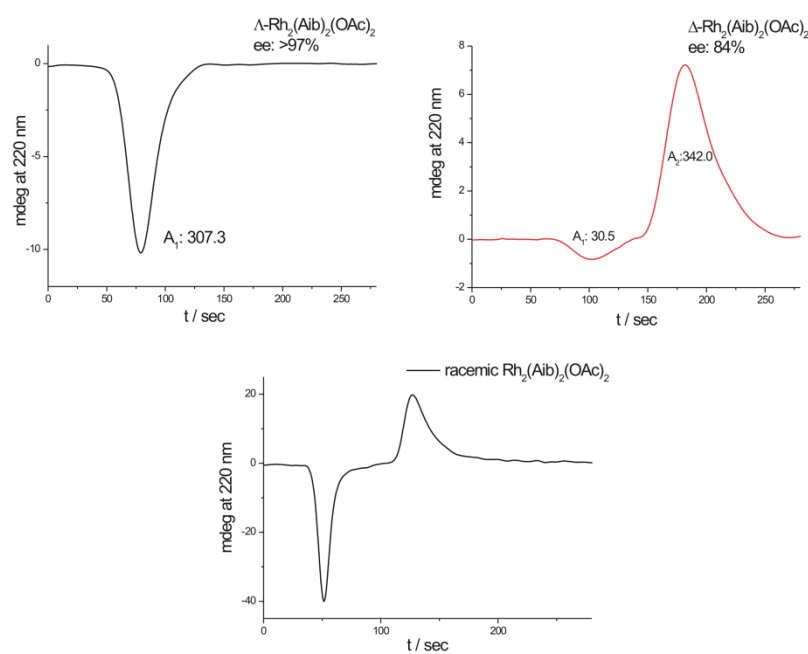


Figure S2. Chiral HPLC-CD separation of the $\text{Rh}_2(\text{Aib})_2(\text{OAc})_2$ complex

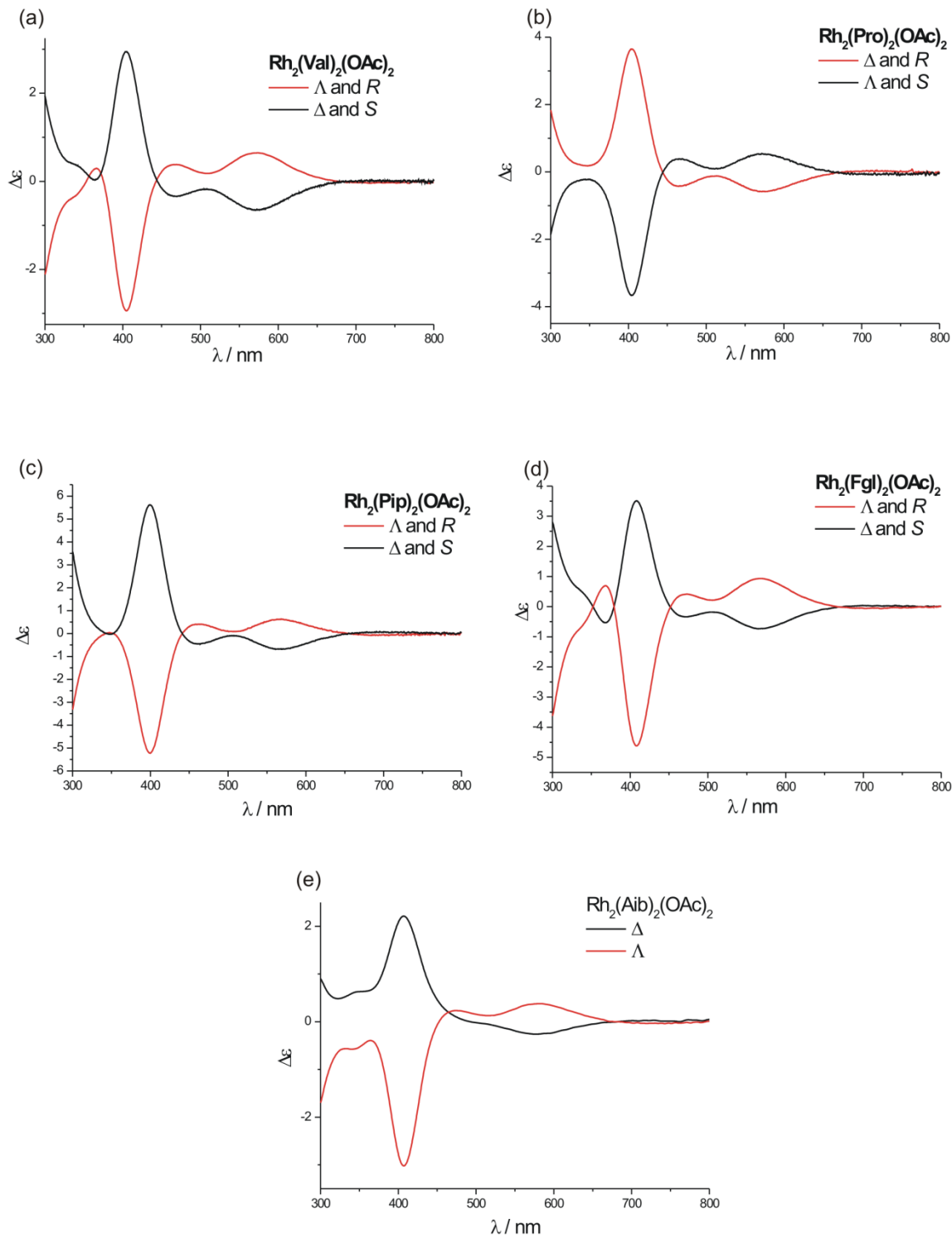


Figure S3. ECD spectra of the chiral complexes (solvent: ACN, c: ~0.4 mg/ml, quartz cell of 10 mm).

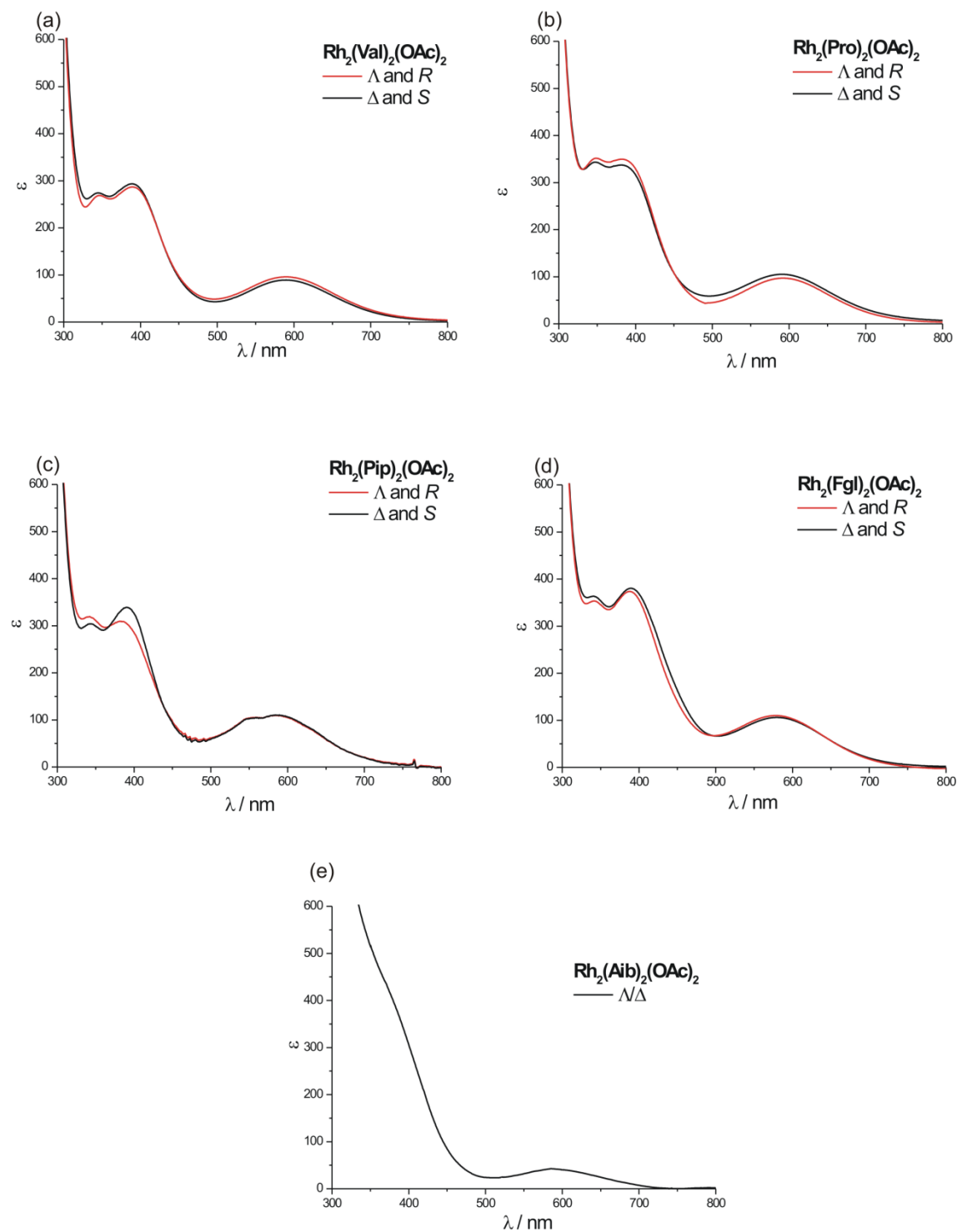


Figure S4. UV-vis spectra of the complexes (ACN, quartz cell of 10 mm, Jasco V-660 spectrophotometer)

Table S1. UV-vis spectroscopic data of the complexes

Complex	λ_{\max} / nm (ϵ / $\text{dm}^3 \cdot \text{mol}^{-1} \cdot \text{cm}^{-1}$)		
Rh ₂ (Val) ₂ (OAc) ₂	589 (89)	389 (291)	346 (272)
Rh ₂ (Pro) ₂ (OAc) ₂	593 (101)	382 (342)	349 (345)
Rh ₂ (Pip) ₂ (OAc) ₂	582 (108)	388 (318)	342 (310)
Rh ₂ (Fgl) ₂ (OAc) ₂	579 (107)	390 (376)	341 (357)
Rh ₂ (Aib) ₂ (OAc) ₂	587 (43)	shoulder	shoulder

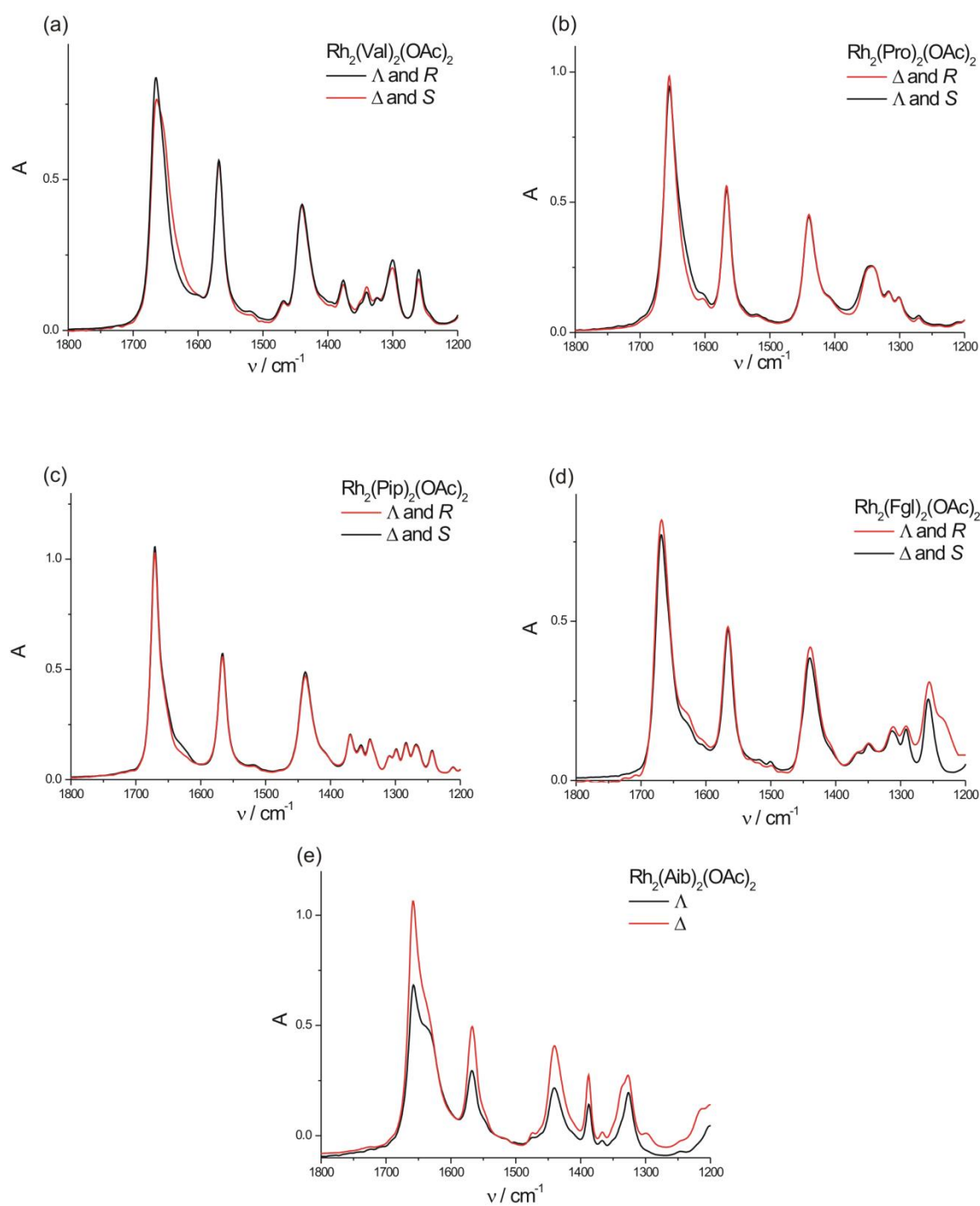


Figure S5. The FT-IR spectra of the chiral complexes (c: 14 mg/ml, ACN-d₃, BaF₂ cell of 0.207 mm).

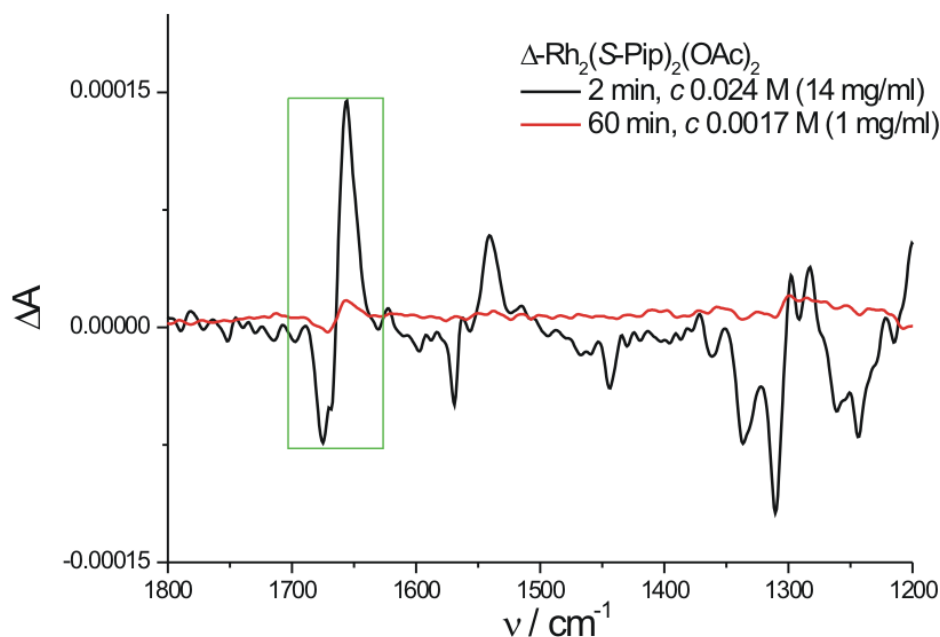
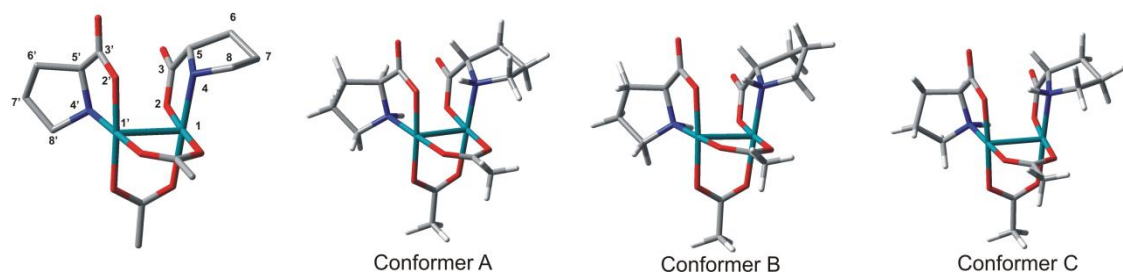


Figure S6. Application of the VCD exciton chirality method for a short and a low-concentration measurement (ACN-d₃, BaF₂ cell of 0.207 mm).

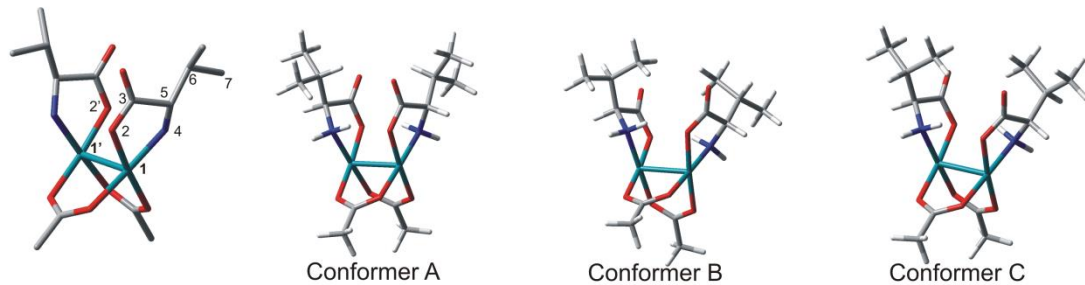
Table S2. Results of population analysis

Compound	Conformer	ΔG (kcal/mol)	Population
$\Delta\text{-Rh}_2(\text{S-Val})_2(\text{OAc})_2$	A	0.000	0.811
	B	0.948	0.163
	C	2.021	0.026
$\Delta\text{-Rh}_2(\text{S-Pro})_2(\text{OAc})_2$	A	0.000	0.528
	B	0.319	0.307
	C	0.689	0.164
$\Delta\text{-Rh}_2(\text{S-Pip})_2(\text{OAc})_2$	A	0.000	1
$\Delta\text{-Rh}_2(\text{S-Pgl})_2(\text{OAc})_2$	A	0.000	0.947
	B	1.695	0.053
$\Delta\text{-Rh}_2(\text{Aib})_2(\text{OAc})_2$	A	0.000	1



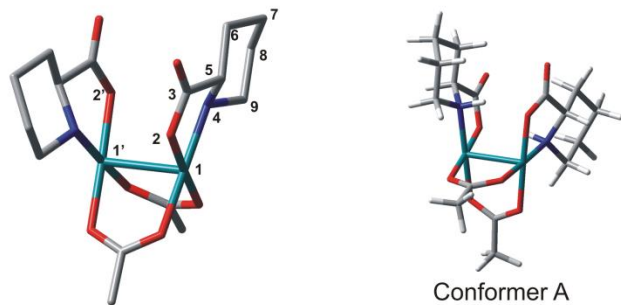
Complex	Conformer	$\alpha(2,1,1',2')$	$\beta(4,5,3,2)$, β'	$\gamma(1,4,5,6)$, γ'	Torsion Angle	$\delta(4,5,6,7)$, δ'	$\varepsilon(5,6,7,8)$, ε'	$\zeta(6,7,8,4)$, ζ'	$\eta(7,8,4,5)$, η'
$\Delta\text{-Rh}_2(\text{S-Pro})_2(\text{OAc})_2$	A	-82	-8, -8	-113, -116	+13, -32	-33, +30	+41, -34	-33, +14	
	B	-81	-7	-115	-32	+40	-34	+14	
	C	-81	-10	-111	+12	-33	+41	-34	

Figure S7. Conformers of $\Delta\text{-Rh}_2(\text{S-Pro})_2(\text{OAc})_2$ complex and their relevant torsion angles



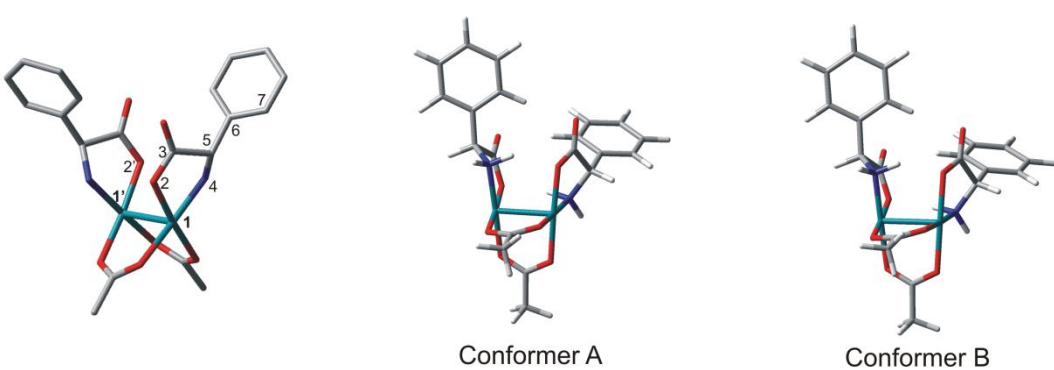
Complex	Conformer	$\alpha(2,1,1',2')$	$\beta(4,5,3,2)$	$\gamma(1,4,5,6)$	Torsion Angle	$\delta(4,5,6,7)$
$\Delta\text{-Rh}_2(\text{S-Val})_2(\text{OAc})_2$	A	+74	+34	-164	-43	
	B	+72	+28	-169	63	
	C	+73	+29	-172	-161	

Figure S8. Conformers of $\Delta\text{-Rh}_2(\text{S-Val})_2(\text{OAc})_2$ complex and their relevant torsion angles



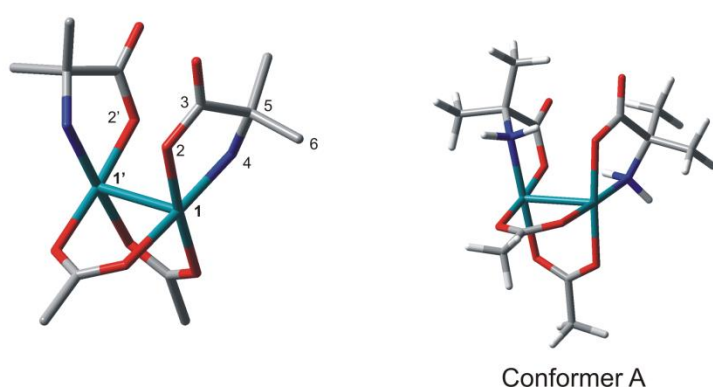
Complex	Conformer	$\alpha(2,1,1',2')$	$\beta(4,5,3,2)$	$\gamma(1,4,5,6)$	Torsion Angle	$\delta(4,5,6,7)$	$\varepsilon(5,6,7,8)$	$\zeta(6,7,8,9)$	$\eta(7,8,9,4)$	$\theta(8,9,4,5)$
$\Delta\text{-Rh}_2(\text{S-Pip})_2(\text{OAc})_2$	A	+75	+33	-165	-57	+53	-52	54	-59	

Figure S9. Conformer A of $\Delta\text{-Rh}_2(\text{S-Pip})_2(\text{OAc})_2$ complex and its relevant torsion angles



Complex	Conformer	Torsion Angle			
		$\alpha(2,1,1',2')$	$\beta(4,5,3,2)$	$\gamma(1,4,5,6)$	$\delta(4,5,6,7)$
$\Delta\text{-Rh}_2(\text{S-Pgl})_2(\text{OAc})_2$	A	+69	+35	-172	-113
	B	+66	+33	-172	-111

Figure S10. Conformers of $\Delta\text{-Rh}_2(\text{S-Pgl})_2(\text{OAc})_2$ complex and their relevant torsion angles



Complex	Conformer	Torsion Angle		
		$\alpha(2,1,1',2')$	$\beta(4,5,3,2)$	$\gamma(1,4,5,6)$
$\Delta\text{-Rh}_2(\text{Aib})_2(\text{OAc})_2$	A	+74	+28	+83

Figure S11. Conformer A of $\Delta\text{-Rh}_2(\text{Aib})_2(\text{OAc})_2$ complex and its relevant torsion angles